

Unveiling the sculpting process of planetary nebulae with the Very Large Telescope

Mónica W. Blanco¹, Martín A. Guerrero¹, Luis F. Miranda^{2,3}, José F. Gómez¹, Hans-Ulrich Käuff⁴, Eric Lagadec⁴, and Olga Suárez⁵

¹ Instituto de Astrofísica de Andalucía - CSIC, Granada, Spain

² Consejo Superior de Investigaciones Científicas, Spain

³ Universidade de Vigo, Departamento de Física Aplicada, Vigo, Spain

⁴ European Southern Observatory, Garching bei München, Germany

⁵ OCA - Université de Nice Sophia Antipolis, Nice, France

Abstract

Planetary nebulae (PNe), the endpoint of the evolution of low- and intermediate-mass stars, display a wild morphological variety. Observations indicate that the onset of asymmetry in PNe already originates at the end of the Asymptotic Giant Branch (AGB) phase or during the post-AGB phase. Therefore, objects in these transition stages provide us a unique opportunity to investigate the sculpting processes of PNe. Here we report VISIR mid-IR high angular resolution observations of a sample of young PNe and objects in their transition to the PN phase. The investigation of the shaping mechanisms requires even higher resolution observations. AMBER and MIDI at the VLTI may provide the required spatial resolution, but the imaging capabilities are limited and the observations are heavily time-consuming. On the other hand, spectro-astrometry using CRIRES-VLT can provide robust results at a lower observational cost. We report preliminary results of our CRIRES spectro-astrometry exploratory program in the search for disks inside PNe.

1 The planetary nebulae phenomenon

The planetary nebula (PN) phenomenon is the remnant produced by low- and intermediate-mass stars ($M_i = 0.8 - 10 M_\odot$). One of the most intriguing aspects in the study of PNe is the amazing variety of morphologies that these objects display, including highly collimated lobes and extremely axisymmetric structures. Previous radio and mid-IR observational studies have provided the first evidences of the onset of asymmetry at some point during the late Asymptotic Giant Branch (AGB) and the post-AGB phases, the immediate precursors of

PNe [20, 23, 7, 2]. The extremely axysymmetric shapes in PNe defy the canonical Generalized Interacting Stellar Wind model (*GISW*, [1]), leading to the proposition of the existence of disks collimating outflows as a basic component to sculpt such morphologies. Possible explanations for the existence of these disks in PNe include binary systems [19] and magnetic fields [5], however, a satisfactory explanation of this phenomenon is still under debate. The observation and detection of disks in PNe represent a challenge because they lay in the cores of PNe, they are compact, and they are often obscured at optical wavelengths. They are, however, bright toward infrared and radio frequencies, and spectroscopic and interferometric observations have found strong evidences of dust and/or gaseous disks at the center of a few proto-PNe (e.g., AFGL 915) and young PNe (e.g., Mz 3 and M2 – 9). Nevertheless, the incapability to produce images and the the strong model dependence to interpret AMBER and MIDI interferometric observations impose serious constrains to the results.

2 VISIR-VLT: Mid-IR high angular resolution imaging

We have obtained VISIR (VLT Imager and Spectrometer for the mid-IR, [8]) data of a sample of young PNe and post-AGB candidates. Table 1 shows the list of objects resolved by VISIR-VLT, as well as the filters and the FWHM obtained for these observations. In sections 2.1 and 2.2 we describe some of the results of our VISIR observations.

Table 1: Objects resolved with VISIR-VLT.

Program ID	Object	Filters ^a	FWHM (arcsecs)
085.D-0256	K 3-35	PAH1, SiC, [S IV]	0.3
087.D-0367	IRAS 15534-5422	PAH1, SiC, [Ne II], Q1	0.35
”	IRAS 17009-4154	PAH1, SiC, [Ne II], Q1	0.36
”	IRAS 18229–1127	PAH1, SiC, [Ne II], Q1	0.42
”	IRAS 18454+0001	PAH1, SiC, [Ne II], Q1	0.35
087.D-0332	IRAS 18061-2525	PAH1, SiC, [Ne II], Q1	0.3

^a The wavelengths corresponding to each filter are: PAH1 $\lambda 8.6 \mu\text{m}$, [S IV] $\lambda 10.4 \mu\text{m}$, SiC $\lambda 11.9 \mu\text{m}$, [Ne II] $\lambda 12.8 \mu\text{m}$, and Q1 $\lambda 17.7 \mu\text{m}$

2.1 The planetary nebula K 3-35

This young PN with bright bipolar lobes separated by a dark lane in the optical and precessing jets detected with VLA radio observations has provided the first evidences of a small-sized (80 AU) magnetized torus of H₂O masers in a PN [10, 11, 22]. The detection of H₂O masers imply an extremely short age for this source, as masers are not expected during the PN phase because the strong UV radiation destroys these molecules [9, 6]. Therefore, the observation of PNe that still harbour H₂O masers (a.k.a. H₂O-PN) represents a unique opportunity to study the youngest PNe.

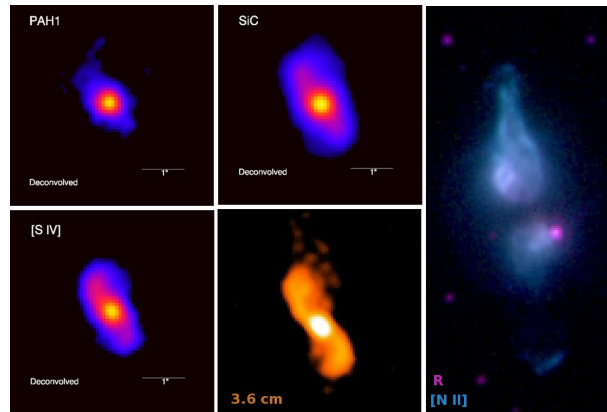


Figure 1: Deconvolved VISIR-VLT N-band (PAH1, SiC, and [S IV]), radio continuum ($\lambda 3.6$ cm), and *HST* WFPC2 optical color-composite (R and [N II]) images of K 3-35.

Our N-Band VISIR images in Fig. 1 display the precessing jets of K 3-35 as a bright S-shaped structure $2.4''$ in size along $PA \sim 30^\circ$ in the SiC and [S IV] images. The PAH1 image resolves the onset of these jets, whereas the SiC image marginally resolves them (Fig. 1). The core of K 3-35 is the brightest region in the N-band and in radio. If we compare the [N II], SiC, and 3.6 cm images, we can infer that the dust emission dominates at the center of this PN and the radio continuum dominates the jets, but also toward the N-band. Thus, most of the mid-IR emission arises from a compact core that encloses the torus of H_2O masers.

2.2 Obscured post-AGB sources

A sample of four post-AGB candidates selected from *Spitzer* IRAC observations has been observed with VISIR-VLT (program: 087.D-0367(A)) and we have resolved with unprecedented detail the morphological characteristics of the extended emission of IRAS 15534–5422, IRAS 17009–4154, IRAS 18229–1127, and IRAS 18454+0001 [3]. These four objects are mostly heavily obscured with weak or no optical counterpart [15, 16]. The VISIR-VLT observations allow us to explore the thermal emission of the dust of this sample of bright mid-IR emitting sources using color (temperature maps) and optical depth maps [4].

Two remarkable examples of this VISIR-VLT imaging study are IRAS 15534–5422 and IRAS 18454+0001 (Fig. 2). In the case of the young bipolar PN IRAS 15534–5422, the images reveal an innermost dusty ring-like innermost structure with ionized small bipolar lobes. This morphological interpretation is supported by its color map constructed with the ratio of a pair of images at two mid-IR wavelengths ([Ne II] and Q1) in which the ring-like structure is the coldest component ($T \sim 100$ K) and the bipolar lobes represent the hottest regions of this source. As for the young PN IRAS 18454+0001, its extended mid-IR emission results in a compact innermost torus or ring of dust embedded in a spherical shell. Its color map is also in concordance with this interpretation, being the dusty torus a cold structure ($T \sim 80$ K) in this PN.

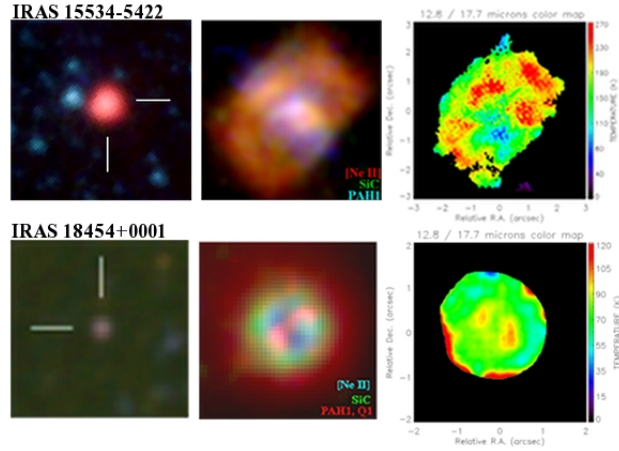


Figure 2: *Spitzer* IRAC image, VISIR RGB composite picture (PAH1, SiC, [Ne II], and Q1), and VISIR color map of IRAS 15534-5422 (*top*) and IRAS 18454+0001 (*bottom*).

Previous studies focused in the transition to the PN phase have provided large samples of sources with extreme axysymmetry as a common characteristic during the proto-PN stage [17, 18, 21]. Our VISIR-VLT imaging study, however, shows only mild asymmetries in heavily obscured sources starting the PN phase. The images and the color maps constructed with VISIR-VLT data further demonstrate the usefulness of mid-IR high resolution observations for the study of this short evolutionary phase.

3 CRIRES-VLT: high resolution spectro-astrometry

To study the shaping mechanism of PNe, it is necessary the high resolution at mas scales provided, for example, by VLTI long baseline interferometry. However, optical and IR interferometry is somehow limited to very bright targets and imposes important constrains in the models to interpret the data. On the other hand, the spectro-astrometry technique offers the possibility of high spatial and spectral resolutions at mas using a single telescope and standard instrumental setup. Spectro-astrometry has already proven its efficiency resolving disks around Be stars [12, 24], and proto-planetary disks of molecular gas with an extraordinary precision: $v=3 \text{ km s}^{-1}$ with a spatial resolution below 1 mas [13, 14].

We have requested and obtained observation time with CRIRES-VLT (CRyogenic high-resolution Infra-Red Echelle Spectrograph) as part of the programs 089.D-0768(A) and 090.D-0761(A) (P.I. M.W. Blanco) to apply for the first time the spectro-astrometry technique in the search for disks in proto-PNe and young PNe with extreme bipolar morphologies. Our observation strategy consists in the observation of atomic and ionic lines such $\text{H}_2 \lambda 2.12 \mu\text{m}$, $\text{Br}\gamma \lambda 2.16 \mu\text{m}$ and $\text{Br}\alpha \lambda 4.05 \mu\text{m}$, as well as molecular lines of $\text{SiO} \lambda 4.04 \mu\text{m}$ and the fundamental band of $\text{CO} \lambda 4.7 \mu\text{m}$. Since spectro-astrometry is extremely sensible to the position angle (PA) observed, we have requested the observation of three or four different PAs accordingly to the axis of symmetry of the source. We have in addition requested the

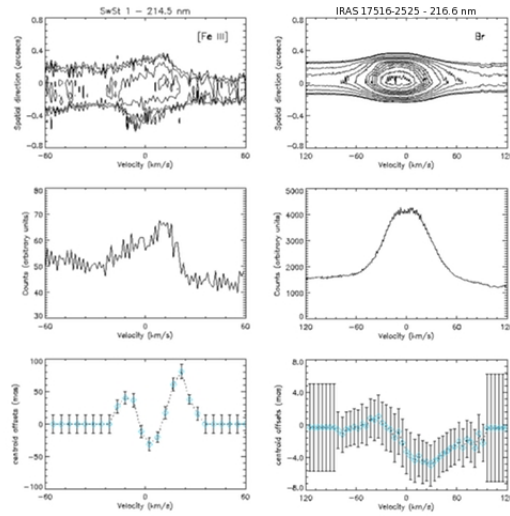


Figure 3: Preliminary spectro-astrometry results obtained with CRIRES commissioning data.

observation of the complementary PA in order to correct for PSF artifacts.

During the first phase of our study we have selected a representative sample of proto-PNe (AFGL 915) and PNe (Mz 3 and M 2-9) with strong evidences of gaseous and/or dusty disks that have produced highly collimated bipolar lobes. Additionally, we have used CRIRES commissioning data to develop the methodology and the tools to perform spectro-astrometry in compact and asymmetric PNe.

3.1 Resolving compact structures using CRIRES spectro-astrometry

To perform the spectro-astrometric analysis of a dispersed spectrum affected by the seeing and recover sub-seeing structures, we measure the offsets of the centroid along the spatial direction at certain wavelength range. This is done by fitting a Gaussian profile, which is a good approximation to the PSF shape. The whole spectral range is scanned with this Gaussian profile with several apertures of 4×50 pixels ($\sim 6 \text{ km s}^{-1}$) along the dispersion axis. Each position of the centroid corresponds to a spatial offset at certain wavelength, thus, sub-seeing spectral features at mas scales are revealed by comparing the spectro-astrometrical signals at different PAs.

Our preliminary spectro-astrometric results in Fig. 3 applied to CRIRES commissioning data of evolved stars suggest the presence of compact structures at mas scales. As for the CO-rich proto-PN SwSt 1, we have detected the spectro-astrometric signal of small bipolar outflows in the [Fe III] line at $2.14 \mu\text{m}$. As for the compact proto-PN IRAS 17516–2525, our analysis suggests an innermost gaseous Keplerian disk detected in the $\text{Br}\gamma$ line at $2.16 \mu\text{m}$. None of these sources had been resolved with this detail before, thus demonstrating the capability of this technique for the study of structural components of PNe at the smallest spatial scales.

References

- [1] Balick, B. & Frank, A. 2002, *ARA&A*, 40, 439
- [2] Blanco, M.W., Guerrero, M.A., Miranda, L.F., Lagadec, E., & Suárez, O. 2012, *IAU Symposium*, 283, 440
- [3] Blanco, M.W., Guerrero, M.A., Ramos-Larios, G., Miranda, L.F., Lagadec, E., Suárez, O., & Gómez, J.F. 2012, submitted to *A&A*.
- [4] Dayal, A., Hoffmann, W.F., Bieging, J.H., et al. 1998, *ApJ*, 492, 603
- [5] García-Segura, G., López, J. A., & Franco, J. 2005, *ApJ*, 618, 919
- [6] Gómez, Y., Moran, J.M., & Rodríguez, L.F. 1990, *RevMexAA*, 20, 55
- [7] Lagadec, E., Verhoelst, T., Mékarnia, D., et al. 2011, *MNRAS*, 417, 32
- [8] Lagage, P. O., Pel, J. W., Authier, M., et al. 2004, *The Messenger*, 117, 12
- [9] Lewis, B.M. 1989, *ApJ*, 338, 234
- [10] Miranda, L.F., Fernández, M., Alcalá, J.M., et al. 2000, *MNRAS*, 311, 748
- [11] Miranda, L.F., Gómez, Y., Anglada, G., & Torrelles, J.M. 2001, *Nature*, 414, 284
- [12] Oudmaijer, R. D., Parr, A. M., Baines, D., & Porter, J. M. 2008, *A&A*, 489, 627
- [13] Pontoppidan, K. M., Blake, G. A., van Dishoeck, E. F., et al. 2008, *ApJ*, 684, 1323
- [14] Pontoppidan, K. M., Blake, G. A., & Smette, A. 2011, *ApJ*, 733, 84
- [15] Ramos-Larios, G., Guerrero, M. A., Suárez, O., Miranda, L. F., & Gómez, J. F. 2009, *A&A*, 501, 1207
- [16] Ramos-Larios, G., Guerrero, M. A., Suárez, O., Miranda, L. F., & Gómez, J. F. 2012, *A&A*, 545, A20
- [17] Sahai, R. & Trauger, J. T. 1998, *ApJ*, 116, 1357
- [18] Sahai, R., Morris, M., Sánchez Contreras, C., & Claussen, M. 2007, *AJ*, 134, 2200
- [19] Soker, N. 1992, *AJ*, 386, 1905
- [20] Suárez, O., Lagadec, E., Bendjoya, P., et al. 2011, *Asymmetric Planetary Nebulae 5 conference*, held in Bowness-on-Windermere, U.K., 20 - 25 June 2010, A. A. Zijlstra, F. Lykou, I. McDonald, and E. Lagadec (eds.) 2011, *Jodrell Bank Centre for Astrophysics*
- [21] Ueta, T., Meixner, M., & Bobrowsky, M. 2000, *ApJ*, 528, 861
- [22] Uscanga, L., Gómez, Y., Raga, A.C., et al. 2008, *MNRAS*, 390, 1127
- [23] Verhoelst, T., Waters, L.B.F.M., Verhoeff, A., et al. 2009, *A&A*, 503, 837
- [24] Wheelwright, H. E., Vink, J. S., Oudmaijer, R. D., & Drew, J. E. 2011, *A&A*, 532, A28